This article has been accepted for publication in a future issue of this journal, but has not been fully edited. Content may change prior to final publication.
Citation information: DOI10.1109/tsg.2022.3153635, IEEE Transactions on Smart Grid

Optimal Operating Regime for Virtual Power Plants Considering Reserve Uncertainty

Han Wang, *Student Member, IEEE*, Youwei Jia, *Member, IEEE*, Chun Sing Lai, *Senior Member, IEEE*, Kang Li, *Senior Member, IEEE*

***Abstract*—Virtual power plant (VPP) has become an important resource for reserve provision owing to its fast-responding capability. In this paper, an optimal VPP operational regime considering reserve uncertainty is proposed, which includes a novel day-ahead offering strategy and a real-time dispatching model. At the day-ahead stage, the offering strategy gives the VPP's price-dependent offers in the energy market under multiple uncertainties on market price, renewable generation, and calls of reserve deployment. A hybrid stochastic minimax regret (MMR) model is proposed to facilitate making offering decisions in the electricity market. At the real-time dispatching stage, generation scheduling can be realized based on the MMR criterion in an online fashion. To alleviate the intrinsic conservativeness of the dispatching model, a self-adaptive algorithm is also proposed to instantly modify the confidence bounds. The proposed regime is comprehensively tested through extensive case studies, of which the simulation results demonstrate the effectiveness in obtaining economic and less conservative offering decisions.**

***Index Terms*— Uncertainty, price-dependent offering strategy, stochastic minimax regret, secondary reserve, self-adaptive**

I. Introduction

GROWING pressure on secured energy supply and environmental issues is now boosting the development of distributed energy resources (DERs) [1]. In the past few decades, both the bulk injection and penetration level of the DERs have been dramatically increased [2]. Moreover, many major energy consumption parties, such as China and the European Union, have recently announced their carbon neutralization plans. In the foreseeable future, the amount of DERs will continue to grow to a great extent.

DER normally features small power capacities and inherent intermittency [3]. From the perspective of the system operator (SO), the massive integration of DERs into the power system will cast great challenges on system operation security [4]. From individual DER point of view, they can hardly access the wholesale market and benefit from the market competition. As a promising solution to the aforementioned occasion, virtual power plants (VPP) can aggregate multiple DERs to become a single market participant with an integrated operating profile [5]. Through such VPP aggregation, the power fluctuations induced by DERs can be absorbed. Moreover, the aggregated DERs can be admitted into the wholesale market for economic operation instead of "free-running".

In electricity markets, joining in multiple markets rather than only the day-ahead energy market has become an efficient approach to improve the profitability of the market participants. In [6], authors develop a multi-market bidding strategy for demand side aggregators participating in a sequential of capacity reserve market, day-ahead, and real-time flexibility markets. In [7], a bidding strategy is proposed for a hydropower producer to participate in both the day-ahead and balancing markets in the NORDPOOL system. In [8], a model predictive control scheme is proposed to enable parallel participation of Denmark demand response providers in both the day-ahead and intraday markets. In [9], authors reviewed optimization models for hydropower producers bidding in multiple markets. It is concluded that participating in multiple markets offers opportunities in the form of possibilities to trade their way to profitable and flexible production schedules.

Owing to the fast-responding capability of the DERs, the VPP is of high potential to arbitrage through the ancillary service markets [10]. In the literature, several attempts have been engaged in VPP operation by considering the provision of reserve. At the early stage, attempts to incorporate reserve provision in VPP operational regime normally focus on developing joint optimization models to maximize the VPP's profit while neglecting the uncertainties. In the works reported in [11] and [12], authors develop an optimization problem to maximize the profit from both selling the energy and proving reserve under no uncertainty. In [13], a more comprehensive model that includes energy, reserve, and reactive power provision is developed to help the VPP arbitrage in multiple markets without uncertainties. Later, the operating strategies of VPPs with reserve become more complex by involving uncertainties in the decision-making process. Whereas in this stage, these works normally concern only the day-ahead stage, and the real-time stage is rarely included. In [14], a modified scenario-based method is proposed to optimize the VPP's day-ahead energy and reserve scheduling decisions in confronting renewable and market price uncertainties. The work in [15] reports a stochastic optimization-based day-ahead scheduling strategy for VPP with multiple uncertainties including renewable generation, market price, and electrical load. In the day-ahead self-scheduling model developed in [16], scenarios and confidence bounds are used to jointly describe the uncertainties in price, wind generation, and reserve calls.

To date, VPP works considering reserve provision become more complete. The gap between the day-ahead stage forecast and the real-time stage information is handled by using multi-stage models. In [17], authors propose a two-stage risk-constrained stochastic optimization model for the VPP energy and reserve scheduling in both day-ahead and real-time stages. In [18], authors study a multi-energy VPP participating in the day-ahead energy and reserve markets. In the intraday operation, adjustments are introduced to the day-ahead baseline schedule with more accurate uncertainty information.

Indeed, researchers have progressed significantly in

Copyright © 2022 IEEE. Personal use of this material is permitted. Permission from IEEE must be obtained for all other uses, in any current or future media, including reprinting/republishing this material for advertising or promotional purposes, creating new collective works, for resale or redistribution to servers or lists, or reuse of any copyrighted component of this work in other works.

This article has been accepted for publication in a future issue of this journal, but has not been fully edited. Content may change prior to final publication.
Citation information: DOI10.1109/tsg.2022.3153635, IEEE Transactions on Smart Grid

studying the VPP's offering and dispatching with reserve. However, most of the existing works concern price-independent offering strategies in the operation of VPPs with reserve. That is, the energy exchange volume is initially fixed regardless of the market-clearing results. Nevertheless, in some electricity markets (e.g., NORDPOOL, PJM, etc.), price-dependent offers can be more effective to reach economic outcomes. In the literature, some preliminary attempts have been made for VPP by deploying the price-dependent energy offering strategy [19], [20]. As compared to price-independent offers, the price-dependent offers are advantageous in reflecting the suppliers' aspiration to sell electricity at different price levels.

Based on the existing literature, this paper aims to develop an optimal VPP operational regime under several uncertainties. The proposed operational regime includes a novel price-dependent offering strategy and a real-time dispatching model. Towards this end, one should firstly resolve the most challenging issue arisen from the uncertainties of market price, renewable generation, and calls for reserve deployment by the SO. Currently, the stochastic optimization approach [15], [21], [22] is widely employed to handle uncertainties in the relevant works of VPP offering. However, in some cases, one can hardly obtain the precise probability distribution for uncertain factors. Hence the effectiveness is obviously limited by solely adopting stochastic optimization. To tackle this issue, hybrid stochastic robust optimization models are proposed (e.g. [16], [23], [24]), in which the probability distribution is unnecessarily needed. However, considerable conservativeness is unavoidable due to the robust nature of these models. As an alternative to handle uncertainties without accurate probability distributions, the MMR approach features distribution-free and less conservative. Thus this method has also been duly deployed in several power engineering applications (e.g., transmission expansion planning in [25], unit commitment problem in [26], and thermal generator bidding problem in [27], etc).

Table I
VPP OPERATIONAL REGIME SUMMARY

References	Price-dependent offering	Real-time dispatch	Reserve provision	Multiple uncertainty models
[10], [21], [28]	-	-	-	-
[19]	√	-	-	-
[29]	-	√	-	-
[11]–[14], [16], [18]	-	-	√	-
[15], [23], [30]	-	-	-	√
[17]	-	√	√	-
[20]	√	-	-	√
This work	√	√	√	√

To emphasize the difference of this work, a summary of VPP operating works is provided in Table I, where four factors are involved for comparison, including price-dependent offering strategy in the day-ahead stage, real-time dispatch, reserve provision, and considering multiple uncertainty models simultaneously.

In the day-ahead offering stage of this work, it is assumed that we have the confidence intervals for renewable generation uncertainty and probability distributions for market price and reserve deployment calls. Hence, on the one hand, confidence bounds are introduced to represent the renewable generation, which serves as a prerequisite input of the MMR model. On the other hand, the market price and uncertain calls for reserve deployment are described by using scenarios complying with certain probability distributions, which enables the utilization of the stochastic optimization model. In combining these two mechanisms, a novel hybrid stochastic MMR model is proposed in this paper to jointly resolve the aforementioned uncertainty issues. In this work, risk-management tools are not considered in the proposed operational regime to maximally reduce the conservativeness in the obtained operating solutions.

At the power dispatching stage and to remain consistent with the MMR-based offering model, a similar mechanism is applied to the scheduling strategy to obtain the optimal VPP dispatching solutions. To control the conservativeness arisen from the minimax nature of the MMR approach, a self-adaptive algorithm is proposed to instantly adjust the confidence interval size based on the revealed uncertainty information.

The contributions of this paper are summarized as follows.

- An optimal VPP operational regime under reserve uncertainty is proposed, which consists of a novel day-ahead price-dependent offering strategy considering uncertain reserve calls and a real-time dispatching model.
- A novel stochastic MMR-based model is proposed for the day-ahead optimal offering decision-makings in VPP.
- A self-adaptive algorithm is proposed to control the conservativeness introduced by the minimax nature of the MMR-based dispatching model in the real-time stage.

The rest of the paper is organized as follows. In Section II, the studied model is discussed in detail. Section III presents the formulations of the optimization problems. The proposed solution methodology and the self-adaptive algorithm are presented in Section IV. Section V provides simulation results and discussions of the case studies. Section VI concludes the work.

II. Model Description

A. Market Structure

The day-ahead energy market adopts a uniform pricing mechanism and the market-clearing resolution is one hour, i.e., there are 24 clearing periods for each day. For each hour, all the energy suppliers are expected to submit stepwise offering curves indicating the amount of energy they are willing to sell at different price levels. In a normal practice, each offering curve comprises at most five steps, namely, five price-quantity pairs. As reported in existing works (e.g. [5], [31]), the dual pricing mechanism is applied for energy deviations at the *ex-post* settlement stage to encourage the suppliers to provide the energy allocated during the bidding process. In this paper, a similar dual pricing scheme (as presented in [5]) is adopted to settle the energy deviations based on market-clearing results. The settlement prices are expressed as follows:

$$\lambda_{m,t}^{+} = \alpha \cdot \lambda_{m,t} \tag{1}$$

$$\lambda_{m,t}^{-} = \beta \cdot \lambda_{m,t} \tag{2}$$

$$\alpha \geq 1 \tag{3}$$

$$\beta \leq 1 \tag{4}$$

where $\lambda_{m,t}$ is the day-ahead energy market-clearing price

This article has been accepted for publication in a future issue of this journal, but has not been fully edited. Content may change prior to final publication.
Citation information: DOI10.1109/tsg.2022.3153635, IEEE Transactions on Smart Grid

at time t; The balancing prices for energy deficit/surplus are given by $\lambda_{m,t}^{+}$ / $\lambda_{m,t}^{-}$, respectively. Parameters α and β are the market penalty coefficients.

B. VPP Operational Model

VPPs are generally equipped with distributed thermal generators, renewable generators like wind turbines (WT) and photovoltaic (PV) panels, as well as energy storage systems. A general block configuration for VPPs is shown in Fig. 1.

The VPP considered in this work participates in the forward reserve market (FRM) and contracts 20% of its dispatchable generation capacity as the secondary reserve. The reserve considered in this work is similar to the thirty-minute reserve [32] in the PJM market except that the resolution has been adjusted to one hour. The VPP receives revenue for providing the potential reserve. Besides, once the reserve is called at a specific operating time, the change in energy production will be settled at the day-ahead market-clearing price. Inversely, failure to deliver the called reserve can result in energy deviations that will be settled in the balancing stage at penalty prices.

In this study, the VPP operation is divided into two stages, i.e., the day-ahead offering stage and the real-time dispatching stage. At the day-ahead offering stage, the VPP is faced with multiple uncertainties relating to energy market price, wind energy generation, and calls for reserve deployment by the SO. At the real-time dispatching stage, the market has been cleared and the SO has informed the VPP of the called reserve volume. Operation uncertainty is all induced by wind power generation at this stage.

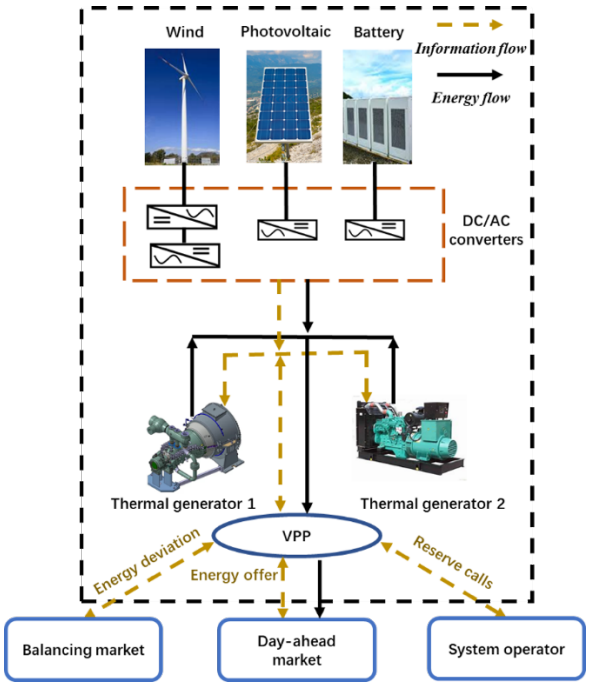

Fig. 1. Configuration of a general VPP.

C. Uncertainty Modeling

In this work, representative scenarios are used to model the wholesale energy market price and calls for reserve deployment. As inspired by [17], a similar scenario generation method is utilized in our study. Since all the offering decisions are made in day-ahead, it is assumed that the probability distribution functions of reserve calls remain unchanged during the next day. Specifically, five typical scenarios are generated for the market price and the reserve deployment uncertainties, respectively. The values of the generated scenarios are ordered as very high, high, medium, low, and very low, which can capture the main features of the price and reserve uncertainty distributions as well as cover most of the possible scenarios in our situation.

To represent the uncertainty induced by wind power generation, confidence bounds are adopted to measure the output range. In our model, the confidence bounds are characterized by a forecasting value u^f and an uncertainty coefficient γ, which indicates the size of the confidence intervals. For given u^f and γ, the real wind power generation u^r is assumed to reside between the bounds expressed as:

$$[(1-\gamma)u^f, \min\{(1+\gamma)u^f, u^{ic}\}] \tag{5}$$

Where u^{ic} is the installed capacity of the renewable generator.

At the offering stage, a constant empirical forecasting accuracy γ^{DA} is considered for all the decision periods because no uncertainty information is revealed in this stage. At the dispatching stage, to reduce the conservativeness stemming from the minimax nature of the dispatching model, the confidence bounds are adjusted by the proposed self-adaptive algorithm based on the uncertainty realizations. The intuition behind the self-adaptive algorithm is that the forecast accuracy of renewable generations is temporally related [33], [34].

III. Model Formulation

To further the discussion in Section II, this section presents detailed formulations for VPP day-ahead offering and real-time dispatching problems, respectively.

A. Day-Ahead Energy Offering

At the day-ahead offering stage, the offering problems of different hours are solved individually. Because three different uncertain factors are considered in this work, a three-level model is proposed to investigate the uncertainties at three different scales. Firstly, the regret model is adopted where only the renewable uncertainty is involved (i.e., Level 1). In concerning both renewable and reserve uncertainties, the stochastic MMR model is formulated (i.e., Level 2). Last, in presence of all operational uncertainties including price uncertainty, the VPP offering curves are formed (i.e., Level 3). The hierarchical structure of the proposed offering strategy is illustrated below and presented in Fig. 2. It is worth mentioning that the optimal offering result obtained from the day-ahead offering model is determined by factors including thermal generator production, renewable generator production, and reserve deployment scenarios.

This article has been accepted for publication in a future issue of this journal, but has not been fully edited. Content may change prior to final publication.
Citation information: DOI10.1109/tsg.2022.3153635, IEEE Transactions on Smart Grid

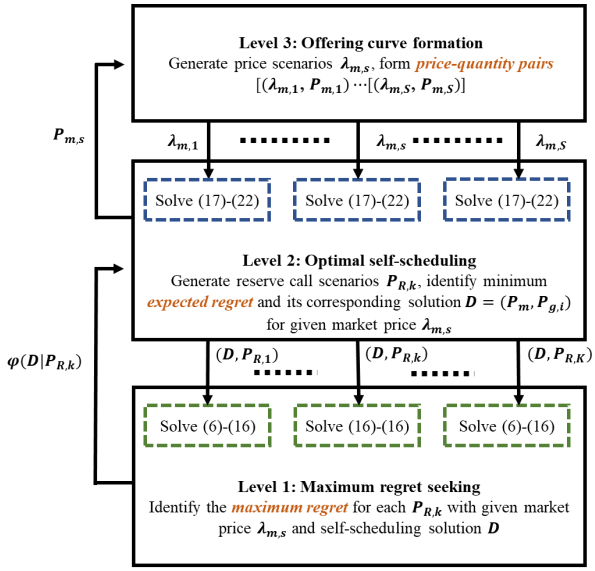

Fig. 2. The hierarchical structure of the day-ahead offering model.

1) Level 1: Regret Maximization

In our problem, regret is defined as the profit difference between the optimal solution with full knowledge of uncertainties and the solution obtained with incomplete information. At this level, both the market-clearing price and the reserve volume requested by the SO are given, the only uncertainty is related to wind power generation. The regret model identifies the worst-case scenario regarding wind uncertainty for a given self-scheduling solution $D = \{P_m, P_{g,i}\}$, where P_m denotes the energy offered in the market and $P_{g,i}$ denotes the power generation of the ith thermal generator.

Given the market-clearing price λ_m and a called reserve volume P_R, the maximum regret $\varphi(D|P_R)$ for the self-scheduling decision D can be acquired by solving the following optimization problem:

$$\max_{u}\left\{\min_{P_m^u, P_{g,i}^u, P_B^u}\left\{\sum_i f^G(P_{g,i}^u) + f^B(P_B^u) - f^M(P_m^u) - f^R(P_R)\right\} - \min_{P_B}\left\{f^M(P_m) + f^R(P_R) - \sum_i f^G(P_{g,i}) - f^B(P_B)\right\}\right\} \tag{6}$$

s.t.

$$(1) - (4) \tag{7}$$

$$f^M(P_m) = \lambda_m P_m \tag{8}$$

$$f^R(P_R) = \lambda_m P_R \tag{9}$$

$$f^G(P_{g,i}) = c_i(P_{g,i})^2 + b_i P_{g,i} + a_i \tag{10}$$

$$f^B(P_B) = \begin{cases} P_B\lambda_m^+, P_B \geq 0 \\ P_B\lambda_m^-, P_B \leq 0 \end{cases} \tag{11}$$

$$P_B^u + \sum_i P_{g,i}^u + \eta u = P_m^u + P_R \tag{12}$$

$$P_B + \sum_i P_{g,i} + \eta u = P_m + P_R \tag{13}$$

$$y_i^u \times P_{g,i}^{min} \leq P_{g,i}^u \leq y_i^u \times P_{g,i}^{max} \tag{14}$$

$$u^f(1-\gamma^{DA}) \leq u \leq \min\{(1+\gamma^{DA})u^f, u^{ic}\} \tag{15}$$

$$y_i^u \in (0,1) \tag{16}$$

The energy offered in the market is denoted as P_m, the power generation of the ith thermal generator is denoted as $P_{g,i}$. Renewable energy production is represented by u and η is the conversion efficiency of the DC/AC converters. The energy deviation is represented by P_B. In this formulation, terms with the superscript u mean that they are optimization variables in the optimal self-scheduling problem under the renewable generation scenario u. The binary variable y_i^u is used to indicate the on/off status of the dispatchable generators. The revenue from the energy market, revenue from responding to the reserve calls, fuel cost of thermal generators, and balancing cost of energy deviations are represented by $f^M(P_m)$, $f^R(P_R)$, $f^G(P_{g,i})$, and $f^B(P_B)$, respectively. Eqs. (12) and (13) are energy balancing constraints in the VPP. Constraints in (14) restrict the power outputs of the thermal generators. Constraint (15) gives the interval for wind power production.

The first inner minimization problem aims to reach the optimal self-scheduling decisions such that the profit of VPP can be maximized under an uncertainty scenario u. The second inner minimization problem is meant to find the optimal recourse action that minimizes the balancing cost under scenario u and first-stage decision D. The overall objective function is the regret of the decision D under the wind generation scenario u. Therefore, the outer maximization problem aims to locate a renewable generation scenario such that the profit difference between the optimal solution and the given solution is maximized.

The regret model presented in this level will be solved multiple times using different reserve deployment scenarios to yield multiple maximum regrets under the wind generation uncertainty. The obtained maximum regrets will be passed to level 2 for further processing.

2) Level 2: Stochastic MMR Model

At level 2, the model is extended to include the uncertain calls for reserve deployment. To this end, scenarios complying with a certain probability distribution are used to represent the reserve call uncertainty. As concerned in the level-1 problem, for a given self-scheduling decision D under the reserve call scenario $P_{R,k}$, its maximum regret $\varphi(D|P_{R,k})$ can be obtained by solving the problem (6) - (16). For a total number of K reserve call scenarios, K regrets can be obtained by solving the problem for K individual times. Since each reserve call scenario corresponds to a certain probability π_k, the 'Expected regret' for the self-scheduling decision D can be obtained by summing up the products of each regret and their corresponding probability. Therefore, the resulting model becomes a hybrid stochastic MMR optimization problem, which aims to make such a decision, of which the expected regret is minimized.

$$\min_D\left\{\varphi(D|P_{R,1}) \times \pi_1 + \cdots + \varphi(D|P_{R,k}) \times \pi_K\right\} \tag{17}$$

s.t.

$$\text{Constraints (6)} - \text{(16)} \tag{18}$$

This article has been accepted for publication in a future issue of this journal, but has not been fully edited. Content may change prior to final publication.
Citation information: DOI10.1109/tsg.2022.3153635, IEEE Transactions on Smart Grid

$$y_i \times P_{g,i}^{min} \le P_{g,i} \le y_i \times P_{g,i}^{max} \quad (19)$$

$$\sum_i P_{g,i} + u^f(1-\gamma^{DA}) \le P_m - P_{R,k} \le \sum_i P_{g,i} + \min\{(1+\gamma^{DA})u^f, u^{ic}\} \quad (20)$$

$$\pi_1 + \cdots + \pi_K = 1 \quad (21)$$

$$y_i \in (0,1) \quad (22)$$

In this formulation, $P_{R,k}$ and π_k are the kth reserve call scenario and its probability. The term $\varphi\left(D|P_{R,k}\right)$ represents the maximum regret of the self-scheduling decision D under the reserve call scenario $P_{R,k}$. Constraints in (19) restrict the power generations of the thermal generators. Constraint (20) limits the energy offer quantity. Constraint (21) ensures that the sum of the reserve call scenario probabilities equals to one.

The stochastic-MMR optimization model presented in this work is solved several times to obtain the optimal offering quantities under different market-clearing price scenarios. The acquired offering quantities will be communicated with level 3 for the final construction of the stepwise offering curve.

Level 3: Offering Curve Formation

At this level, to handle the price uncertainty, price scenarios ranging from low to high are generated to represent different price levels. The generated price scenarios are used as the bidding prices in the stepwise bidding curves, and the bidding volumes corresponding to each price scenario can be obtained by solving problem (17) – (22) independently for each price scenario. As S price scenarios are considered as the input of problem (17) – (22), the same number of price-quantity pairs can be acquired. By combining the obtained price-quantity pairs, the offering curves can be hereby constructed.

It should be noted that the order we follow to explain the model is inverse to the actual implementation order of it for ease of understanding. Hence, starting from level 3, the price uncertainty is firstly addressed by generating different price scenarios to form the offering curves, then the reserve deployment uncertainty is addressed by the stochastic optimization in level 2. Finally, level 1 deals with the wind generation uncertainty using the regret model.

B. Real-Time Dispatching

The market-clearing results are passed from the day-ahead stage to the real-time stage. At the real-time stage, the SO has also informed the VPP of the called reserve volume. Hence, thermal generators shall be duly dispatched given the wind generation uncertainty to meet both the day-ahead market-clearing results and the real-time reserve deployment requests.

The MMR-based dispatching problem is formulated as follows:

$$\min_{P_{g,i,t}}\left\{\sum_i f^G\left(P_{g,i,t}\right) + \max_{u_t}\left\{\min_{P_{B,t}} f^B\left(P_{B,t}\right) - \min_{P^u_{g,i,t}, P^u_{B,t}}\left\{\sum_i f^G\left(P^u_{g,i,t}\right) + f^B\left(P^u_{B,t}\right)\right\}\right\}\right\} \quad (23)$$

s.t.

$$\text{Constraint } (7) - (11) \quad (24)$$

$$y^u_{i,t} \times P^{min}_{g,i,t} \le P^u_{g,i,t} \le y^u_{i,t} \times P^{max}_{g,i,t} \quad (25)$$

$$y_{i,t} \times P^{min}_{g,i,t} \le P_{g,i,t} \le y_{i,t} \times P^{max}_{g,i,t} \quad (26)$$

$$-RD_i \le P_{g,i,t+1} - P_{g,i,t} \le RU_i \quad (27)$$

$$-RD_i \le P^u{}_{g,i,t+1} - P^u{}_{g,i,t} \le RU_i \quad (28)$$

$$P^u_{m,t} + P_{R,t} = \sum_i P^u_{g,i,t} + P^u_{B,t} + u_t \quad (29)$$

$$P_{m,t} + P_{R,t} = \sum_i P_{g,i,t} + P_{B,t} + u_t \quad (30)$$

$$u^f_t(1-\gamma^{RT}_t) \le u_t \le \min\{(1+\gamma^{RT}_t)u^f_t, u^{ic}\} \quad (31)$$

$$[y^u_{i,t}, y_{i,t}] \in (0,1) \quad (32)$$

In this formulation, RD_i and RU_i represent the ramp down / up limits of the ith thermal generator. The size of the renewable confidence interval given in (31) will be continuously adjusted by the proposed self-adaptive algorithm presented in the next section.

IV. Solution Methodology

The column-and-constraint-generation (C&CG) algorithm [35] has been proven efficient for solving two-stage minimax problems, yet it cannot be directly applied to the formulated MMR models because of the extra step that is needed to locate the "optimal solution" under scenario u. Hence, in this section, a reformulation methodology is firstly proposed to transform the offering and dispatching problems into two-stage robust optimization problems, then a detailed C&CG framework is developed to solve the reformulated problems. The proposed self-adaptive algorithm is given at the end of this section.

A. Problem Reformulation

It can be observed that both the offering and dispatching minimax regret optimization problems can be written in the following compact form:

$$\min_y\left\{f_1(y) + \max_u\left\{\min_x f_2(x) - \min_{y^u,x^u}\{f_1(y^u) + f_2(x^u)\}\right\}\right\} \quad (33)$$

s.t.

$$Ay \le p, y \in S_Y \quad (34)$$

$$By + Cx - Du \le q \quad (35)$$

$$Ay^u \le p, y^u \in S_Y \quad (36)$$

$$By^u + Cx^u - Du \le q \quad (37)$$

$$Eu \le l, u \in S_U \quad (38)$$

Where y represents the first-stage decision variables. The recourse actions are represented by x. The uncertainty scenario is represented by u and the optimal solution under the uncertainty realization u is given by (y^u, x^u). The negative utility functions of the first- and second-stage variables are given by $f_1(y)$ and $f_2(x)$, respectively.

Proposition: Given that the recourse action solution set is always non-empty, problem (33) – (38) is equivalent to the following two-stage robust optimization problem:

$$\min_y\left\{f_1(y) + \max_\xi\left\{\min_x\{f_2(x) - f_1(y^u) - f_2(x^u)\}\right\}\right\} \quad (39)$$

s.t.

This article has been accepted for publication in a future issue of this journal, but has not been fully edited. Content may change prior to final publication.
Citation information: DOI10.1109/tsg.2022.3153635, IEEE Transactions on Smart Grid

$$(34), (35) \tag{40}$$

$$E'\xi \le l' \tag{41}$$

$$\xi = [u^T, (y^u)^T, (x^u)^T]^T \tag{42}$$

$$E' = \begin{bmatrix} 0 & A & 0 \\ -D & B & C \\ E & 0 & 0 \end{bmatrix} \tag{43}$$

$$l' = \begin{bmatrix} p \\ q \\ l \end{bmatrix} \tag{44}$$

Proof: The reformulation can be completed through the following steps:

$$\min_y \left\{ f_1(y) + \max_u \left\{ \min_x f_2(x) - \min_{y^u, x^u} \{ f_1(y^u) + f_2(x^u) \} \right\} \right\} \tag{45}$$

$$\equiv \min_y \left\{ f_1(y) + \max_u \left\{ \max_{y^u, x^u} \{ -f_1(y^u) - f_2(x^u) \} + \min_x f_2(x) \right\} \right\} \tag{46}$$

$$\equiv \min_y \left\{ f_1(y) + \max_{u, y^u, x^u} \left\{ \min_x \{ f_2(x) - f_1(y^u) - f_2(x^u) \} \right\} \right\} \tag{47}$$

By considering a lifted uncertain vector ξ as displayed in (42), which satisfies constraints (41) - (44), problem (47) can be reformulated into a two-stage robust optimization problem.

B. C&CG Framework

To solve the problem (39) – (44), a detailed C&CG framework is developed in this subsection. Under the C&CG framework, the original problem will be decomposed into primary and secondary problems. In this paper, the primary problem is meant to find the optimal first-stage decisions that will minimize the maximum regret, and it can be written as:

$$\min_{y, \vartheta} \{ f_1(y) + \vartheta \} \tag{48}$$

s.t.

$$(34) \tag{49}$$

$$\vartheta \ge -H \tag{50}$$

$$By + Cx_{v+1} - Du_v^c \le q \tag{51}$$

$$\vartheta \ge f_2(x_v) - f_1(y_v^{u,c}) - f_2(x_v^{u,c}) \tag{52}$$

$$x_{v+1} \in S_X \tag{53}$$

Where ϑ is the auxiliary variable. Variables x_{v+1} are new variables created in the $(v+1)th$ iteration. Terms u_v^c, x_v^c, $y_v^{u,c}$, and $x_v^{u,c}$ are the optimal values calculated in the vth iteration from the secondary problem. The symbol H represents a big enough number to ensure that the primary problem is bounded in the first iteration. Note that in the first iteration, only constraints (49) and (50) are considered.

Since the primary problem is a relaxation of the original problem, its optimal objective value will be no bigger than the actual optimal objective value of the original problem. Therefore, the lower bound will be updated after solving the primary problem:

$$LB = \max \{ LB, f_1(y_{v+1}^c) + \vartheta_{v+1}^c \} \tag{54}$$

Where y_{v+1}^c and ϑ_{v+1}^c represent the optimal primary problem solutions calculated in the $(v+1)th$ iteration.

There are two purposes for the secondary problem, one is to identify the worst-case condition that will maximize the regret of the primary problem decisions, the other is to determine the optimal recourse actions under the worst-case scenario. Using the results obtained from the primary problem, the secondary problem can be formulated as:

$$\theta = \max_\xi \left\{ \min_x \{ f_2(x) - f_1(y^u) - f_2(x^u) \} \right\} \tag{55}$$

s.t.

$$(41) – (44) \tag{56}$$

$$By_{v+1}^c + Cx - Du \le q \tag{57}$$

Where θ represents the maximum value of the secondary problem. Compared to the original problem, the feasible domain of the secondary problem is more restricted, and the optimal objective value of the secondary problem is no less than that of the original problem. Thus, the upper bound can be obtained by solving the secondary problem:

$$UB = \min \{ UB, f_1(y_{v+1}^c) + \theta_{v+1}^c \} \tag{58}$$

The convergence of the problem can be declared once the following criterion is satisfied:

$$UB - LB \le \varepsilon_{ccg} \tag{59}$$

Where the convergence threshold of the C&CG algorithm is given by ε_{ccg}. The complete solution algorithm is provided in algorithm 1.

Algorithm 1 C&CG solution algorithm

1: **Initialize** $v = 0$, $UB = \infty$, $LB = -\infty$, $\varepsilon_{ccg} = 0.001$
2: **While** (62) **is false**, $v \leftarrow v + 1$ **do**
3: Solve (48) – (53), derive $(y_{v+1}^c, \vartheta_{v+1}^c)$ and update the lower bound using (54).
4: Solve (55) – (57), derive $(x_{v+1}^c, y_{v+1}^{u,c}, x_{v+1}^{u,c}, \theta_{v+1}^c)$ and update the upper bound using (58).
5: Create x_{v+1}, add (51), (52), and (53) to the primary problem.
6: **end while**
7: **Return** y_{v+1}^c

As referred to [35], the developed C&CG framework will converge in $O(Q)$ iterations, where Q is the number of extreme points of the renewable generation uncertainty set.

C. Self-Adaptive Algorithm

Due to the minimax nature of the MMR approach in the real-time stage, the dispatch solutions will inevitably be conservative if the confidence intervals are too big. To obtain more economic dispatch solutions, this section proposes an effective look-back-and-adjust self-adaptive algorithm that can reduce the size of the confidence intervals. By observing the past wind uncertainty realizations, the optimal uncertainty coefficient that minimizes the total profit loss of the n previous time windows will be identified and used at the current decision period.

This article has been accepted for publication in a future issue of this journal, but has not been fully edited. Content may change prior to final publication.
Citation information: DOI10.1109/tsg.2022.3153635, IEEE Transactions on Smart Grid

Based on the revealed uncertainty information (i.e., the actual renewable production u^r), the optimal uncertainty coefficient γ that minimizes the total profit loss of the n previous decision periods can be obtained by solving the consensus optimization problem under the alternating direction method of multipliers (ADMM) framework. In this framework, the primary problem is meant to address the conflicts between different time windows, and the secondary problems are designed to locate their own optimal uncertainty coefficient γ. The self-adaptive process is summarized as follows:

1) Select proper values for ρ and $\boldsymbol{\varsigma}^0$, set $v = 0$.

2) Identify such an overall uncertainty coefficient γ that will coordinate the optimal uncertainty coefficients γ_τ for the n previous time windows:

$$\gamma^{v+1} = \underset{\gamma^{v+1}}{\operatorname{argmin}}[\sum_{\tau=t-n}^{t-1}(\gamma^{v+1} - \gamma_\tau^v)^2 + \frac{\rho}{2}\sum_{\tau=t-n}^{t-1}(\gamma^{v+1} - \gamma_\tau^v - \boldsymbol{\varsigma}^v)^2] \tag{60}$$

3) For each past time window, using the revealed uncertainty information and the calculated optimal overall uncertainty coefficient γ^{v+1} to concurrently minimize the energy imbalance cost and the difference between the optimal single window γ_τ^{v+1} and the overall optimal γ^{v+1}:

$$\gamma_\tau^{v+1} = \underset{\gamma_\tau^{v+1}}{\operatorname{argmin}}[f^B(P_B^\tau) + \frac{\rho}{2}(\gamma^{v+1} - \gamma_\tau^{v+1} - \boldsymbol{\varsigma}^v)^2], P_B^\tau \propto u_\tau^f \gamma_\tau^{v+1}, \forall\tau \in [t-n, t-1] \tag{61}$$

4) Update the residual $\boldsymbol{\varsigma}^{v+1}$ using the optimized solutions from problems (60) and (61):

$$\boldsymbol{\varsigma}^{v+1} = \boldsymbol{\varsigma}^v - (\gamma^{v+1} - \gamma_\tau^{v+1}) \tag{62}$$

5) Check the convergence by verifying if the residual change is small enough:

$$\sqrt{(\boldsymbol{\varsigma}^{v+1} - \boldsymbol{\varsigma}^v)^2} \le \varepsilon_{admm} \tag{63}$$

6) If the problem has converged, then the optimal overall uncertainty coefficient can be obtained as γ^{v+1}. Otherwise, update the iteration number to $v = v + 1$ and go back to step 2.

Where the penalty factor, residual, and convergence threshold in the ADMM method are given by ρ, $\boldsymbol{\varsigma}$, and ε_{admm}, respectively. The process for selecting the optimal uncertainty coefficient is illustrated in Algorithm 2.

Algorithm 2 Self-adaptive algorithm for selecting the optimal γ

Initialize $v = 0$, $\boldsymbol{\varsigma}^0 = 0$, $\rho = 100$, $\varepsilon_{admm} = 0.001$, $\gamma_\tau^0 = \frac{|u_\tau^r - u_\tau^f|}{u_\tau^f}$.
While (63) **is false**, $v \leftarrow v + 1$ **do**
    Solve (60) with $(\gamma_\tau^v, \boldsymbol{\varsigma}^v)$ to obtain γ^{v+1}.
    Solve (61) for each past time window parallelly with $(\gamma^{v+1}, \boldsymbol{\varsigma}^v)$ to obtain γ_τ^{v+1}.
    Update $\boldsymbol{\varsigma}^{v+1} \leftarrow \boldsymbol{\varsigma}^v - (\gamma^{v+1} - \gamma_\tau^{v+1})$.
end while
Return γ^{v+1}

V. Case Study

This section provides the numerical results to demonstrate the performance of the proposed operational regime for VPPs.

A. Basic Data

The VPP under study is composed of two thermal generators and one wind generator. Battery is not considered in the case study due to its high investment costs. The generator characteristics are presented in Table II. The Finland day-ahead market price and called reserve volume data from the NORDPOOL market [36] are used. The renewable generation data is the scaled wind generation from Finland [37]. The penalty coefficients α and β are set to be 1.5 and 0.5, respectively. At the day-ahead and real-time stages, the empirical worst-case uncertainty coefficients are set to be 0.7 and 0.4, respectively. In the real-time stage, three look-back time windows are considered.

Table II
GENERATOR CHARACTERISTICS

	P_{max} (MW)	$EcoP_{min}$ (MW)	RU	RD	a $\$/h$	b $\$/MWh$	c $(\$/MWh)^2$
Diesel	45	5	25	15	708	30.7	0.77
Gas	55	5	35	25	531	34.2	0.83
Wind	60	0	/	/	/	/	/

Fig. 3a gives the day-ahead wind forecast data, where the uncertainty coefficient is constant; Fig. 4b shows the real-time wind forecast data, where the uncertainty coefficient is continuously modified.

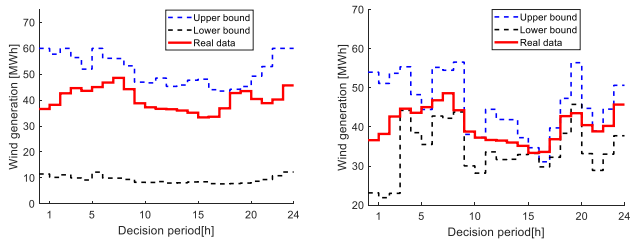

Fig. 3. The actual data and the day-ahead (a) as well as real-time (b) forecast intervals for wind generation.

The market accepts offering curves with at most five steps. Hence, five price-quantity pairs are required in each market-clearing period to construct the offering curve. Because each offering step is obtained by a price scenario and its corresponding offering quantity, five price scenarios are generated for each market-clearing hour to yield five price-quantity pairs. The actual price and generated price scenarios are presented in Fig. 4.

This article has been accepted for publication in a future issue of this journal, but has not been fully edited. Content may change prior to final publication.
Citation information: DOI10.1109/tsg.2022.3153635, IEEE Transactions on Smart Grid

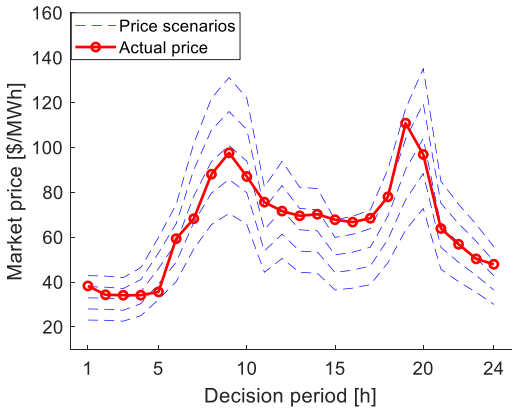

Fig. 4. Generated price scenarios and the actual price.

B. Results and Discussions

The computation platform is AMD Ryzen 8-3700X 3.60 GHz with 16G RAM. The averaged total computation time is 1,424s, which is acceptable under the time scales of day-ahead offering (i.e., multiple hours) and real-time dispatching (i.e., within one hour).

The stepwise energy offers of the VPP in several representative hours are depicted in Fig. 5. In hour 3, the forecast price is low and the VPP is only willing to offer the energy from the wind generator for the first 3 price scenarios. As the price increases, the VPP starts to offer energy generated by the thermal generators for the fourth and fifth price scenarios. Therefore, three offering steps are constructed for hour 3. In hour 15, the forecast price is medium and for each price scenario, the VPP has a corresponding energy offer. In hour 21, the forecast price is high and the VPP is willing to offer its maximum capacity at the fourth price scenario. Though the fifth price scenario is higher than the fourth scenario, the VPP cannot offer more energy to the market, thus, only four steps in hour 21 can be observed.

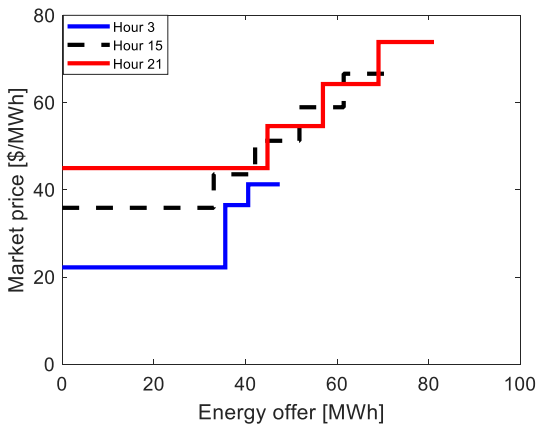

Fig. 5. Offering curves for hours 3, 15, and 21.

According to the market-clearing prices, the accepted VPP energy offers together with the called reserve are displayed in Fig. 6. The required energy is the sum of the market allocated energy and the reserve volume called by the SO.

Fig. 7 displays the dispatching decisions of the thermal generators over the day. In Fig. 7, the VPP does not turn on the thermal generators in hours 1 to 5 and 24 because the market prices are very low. In hours 13, 21 to 23, only the diesel generator remains online, the gas generator is turned off due to its higher variable cost. In hours 12 and 14, both the diesel and gas generators are not generating at their optimal power because of the minimum economic minimum power restriction. It should be noted that, in Fig. 7, the scheduled generation levels do not exactly match the market price levels. For example, the market price at hour 19 is the highest over the day, while the production at hour 19 is not the highest. This violation is due to the VPP needs to respond to the SO's calls for reserve deployment. Therefore, the VPP may curtail its production even at high price hours as shown in Fig. 14.

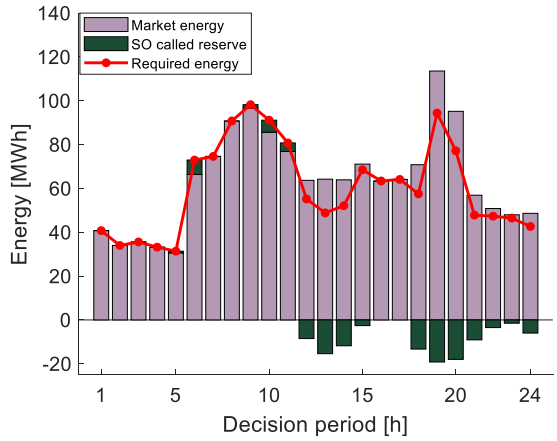

Fig. 6. The market allocated energy, called reserve, and required energy.

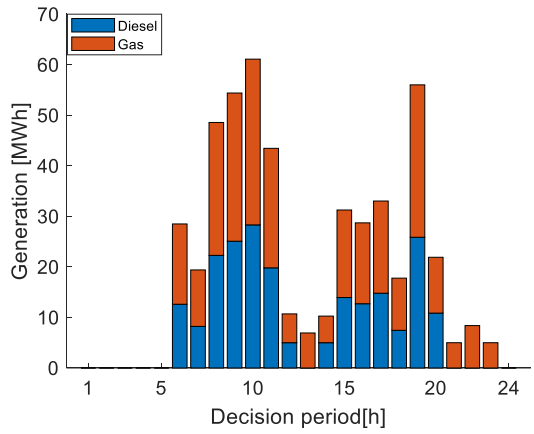

Fig. 7. The dispatching results of the thermal generators.

The hourly net profit and the details of the profit components of the VPP are shown in Fig. 8. The question of how to participate in the FRM is out of the scope of this paper; thus, the revenue in the FRM is not presented here. Due to the existence of the reserve contract, the VPP must respond to the reserve calls from the SO, which induced 6,156$ of revenue loss. The most important revenue is from selling energy to the day-ahead market (92,875$), and the major cost comes from the thermal generator fuel costs (45,179$). The total cost in the balancing market is 3,444$, and the overall operational profit from the proposed operational regime is 38,096$.

To evaluate the economic performance of the proposed operational regime (Case 1), multiple approaches and models are also tested for the VPP under study. The results from the price-dependent offering using the stochastic robust

This article has been accepted for publication in a future issue of this journal, but has not been fully edited. Content may change prior to final publication.
Citation information: DOI10.1109/tsg.2022.3153635, IEEE Transactions on Smart Grid

optimization (RO) model (Case 2), the price-dependent offering using the multistage stochastic programming approach (Case 3), the price-independent offering using the stochastic MMR model (Case 4), and the price-dependent offering using the stochastic MMR model without performing real-time dispatch (Case 5) are provided in Fig. 9 to Fig. 12. The daily profit results of the discussed strategies are summarized in Table III.

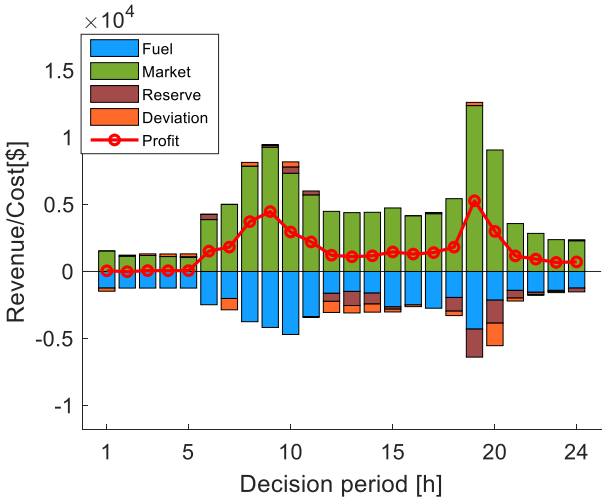

Fig. 8. The VPP's profit using the proposed stochastic MMR model under the price-dependent framework.

Table III
PROFIT RESULTS OF THE THREE STRATEGIES

Operating strategy	Energy market revenue [$]	Fuel cost [$]	Deviation Cost [$]	Net profit [$]
Case 1	92,875	45,179	3,444	38,096 (100%)
Case 2	65,765	32,809	−2,514	29,314 (76.95%)
Case 3	93,450	45,547	3,556	38,191 (100.25%)
Case 4	76,121	35,187	2,338	32,440 (85.15%)
Case 5	92,875	60,982	-9,986	35723 (93.77%)

First, the stochastic MMR optimization model is replaced with the stochastic RO model while maintaining everything else unchanged. Since the offering decisions of different hours are independent of each other, the considered budget of uncertainty in the stochastic RO approach is set to be one.

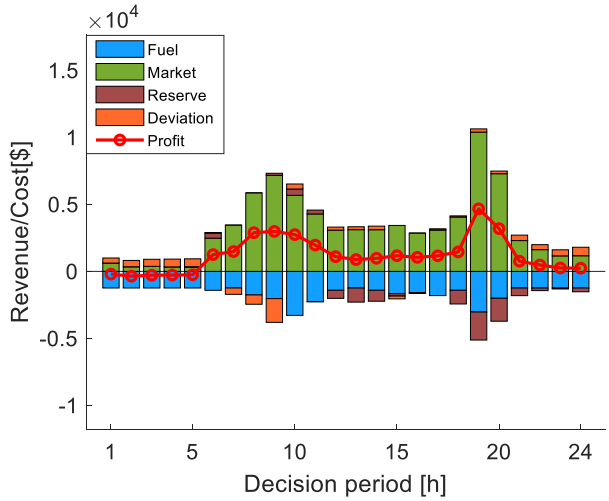

Fig. 9. The VPP's profit using the stochastic RO model under the price-dependent framework.

The VPP's revenue from the energy market is 65,765$. Compared to the revenue (92,875$) obtained when using the stochastic MMR model, one can see that the stochastic RO model offers less energy in the electricity market for the same price levels. The overall profit obtained from the stochastic RO model is 29,314$, which is only 76.95% of the profit when the stochastic MMR model is used. Therefore, one can conclude that, compared to the stochastic RO model, the proposed stochastic MMR model can significantly improve the economic performance of the VPP. Also, it can be observed that the deviation cost is negative, which means that the revenue in the balancing market is larger than the cost. This result confirms that the performance of the stochastic RO model is very conservative and leads to significant positive energy deviations.

To further demonstrate that the proposed method can provide less-conservative solutions without the accurate probability distribution of wind uncertainty, the multistage stochastic programming approach is applied to the VPP under study. In stochastic programming, we remove the restriction that the accurate probability distribution of wind uncertainty is not available and model it by using scenarios instead of confidence intervals. From the result in Table III, one can see that our method performs very closely to the stochastic programming approach. The overall profit by using the proposed method has been merely reduced by 0.25% compared to the multistage stochastic programming approach. The major reason for this difference is that the stochastic programming approach has more precise information that enables it to handle the wind uncertainty by using expected values as the objective, whereas the proposed method only has less-precise information and needs to deal with wind uncertainty based on the minimax criterion. As a result, the conservativeness in the offering and dispatching solutions of the proposed method has been increased slightly compared with the multi-stage stochastic optimization approach.

This article has been accepted for publication in a future issue of this journal, but has not been fully edited. Content may change prior to final publication.
Citation information: DOI10.1109/tsg.2022.3153635, IEEE Transactions on Smart Grid

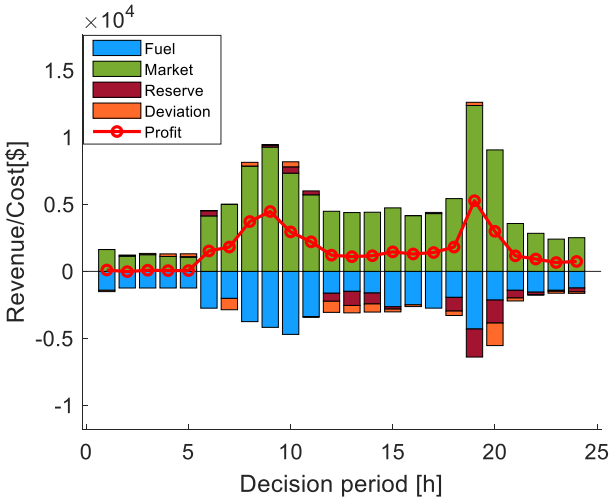

Fig. 10. The VPP's profit using the multistage stochastic programming approach.

Then, to evaluate the difference between price-dependent and price-independent offering strategies, in the price-independent offering using the stochastic MMR model, a single offering profile is generated by using the expected market price. Compared to the price-dependent offering strategy, the price-independent offering strategy is less capable of capturing the arbitraging strategies due to lack of flexibility. This effect is obvious when the market price significantly deviates from the expected price, such as in hours 15, 16, and 19, the ratios of the price-independent strategy profit to the price-dependent strategy profit are 60.28%, 70.85%, and 70.89%, respectively. As a result, the overall profit using the price-independent strategy (32,440$) only takes up 85.15% of the price-dependent strategy profit.

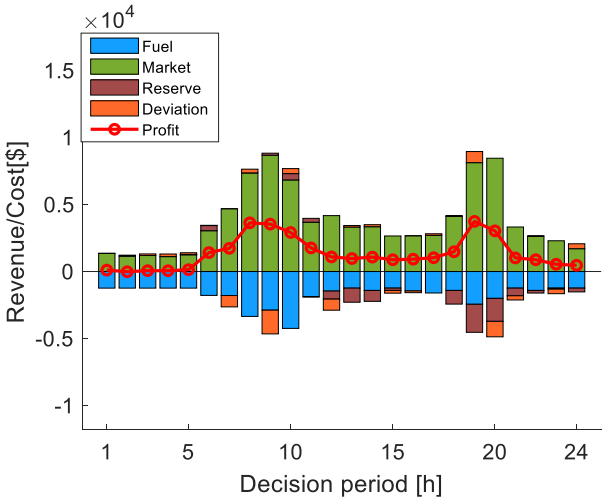

Fig. 11. The VPP's profit using the proposed stochastic MMR model under the price-independent framework.

The impact of doing the real-time dispatch is illustrated by comparing Fig. 12 with Fig. 8, it is easy to notice that the generation cost has been increased when the real-time dispatch is not considered. This is because, with less accurate wind power production prediction, the day-ahead dispatching result is more conservative, which leads to overproduction of the thermal generators. The overproduced energy can only be sold at penalty prices and cause losses in the overall VPP profit.

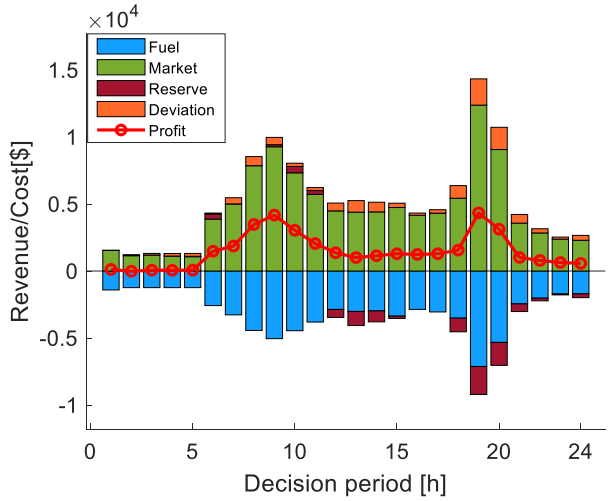

Fig. 12. The VPP's profit using the proposed price-dependent stochastic MMR model without performing real-time dispatch.

To illustrate the effectiveness of the proposed self-adaptive algorithm, the same dispatching problem is solved using both the adjusted and unadjusted uncertainty coefficients. Fig. 13 shows the hourly profit loss using both uncertainty coefficients. The profit losses are obtained by subtracting the profits of the imperfect dispatching solutions from the profits of the perfect information approach [38]. For most of the time, the profit loss from using the adjusted uncertainty coefficient is significantly lower than using the constant worst-case uncertainty coefficient. However, in hour 20, the VPP's profit loss using the adjusted γ is larger than using the worst-case γ, this is because the adjusted confidence bounds failed to contain the real wind generation scenario, as shown in Fig. 4b. This failure is due to the tradeoff that is made between robustness and economic performance. Though larger profit loss may be induced in some hours, the overall profit loss in the dispatching stage using the adjusted γ is 3,280$, which is only 32.34% of the profit loss when using the constant worst-case γ (10,143$).

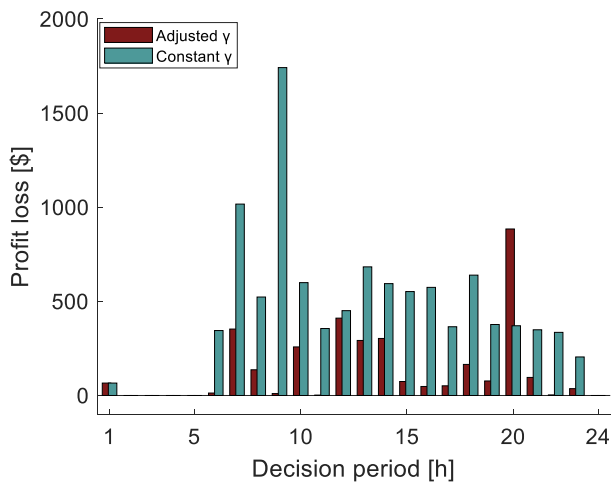

Fig. 13. Profit loss in the dispatching stage using the adjusted and constant uncertainty coefficients.

This article has been accepted for publication in a future issue of this journal, but has not been fully edited. Content may change prior to final publication.
Citation information: DOI10.1109/tsg.2022.3153635, IEEE Transactions on Smart Grid

The reserve response result is presented in Fig. 14 which shows that for most of the time, the VPP can exactly complete the reserve requests from the SO. However, the VPP's capability for reserve deployment is also limited at some hours. When the price is very low, the thermal generators are either offline or producing at minimum economic power. Hence, the VPP cannot flexibly change its power output to complete the reserve calls, such as hours 5, 23, and 24. Similar limitations can also happen when the market price is exceptionally high. Another situation that can limit the VPP's reserve provision capability is large price differences between adjacent hours, which happened at hours 20 and 21. Because most of the ramping capability is used to fulfill the market-clearing results, the flexibility left for responding to reserve calls is not enough to complete the task. The frequency of observing such limitations depends on how often the aforementioned extreme scenarios will happen in the energy market. In total, the VPP completed 91.29% of the requested reserve volume.

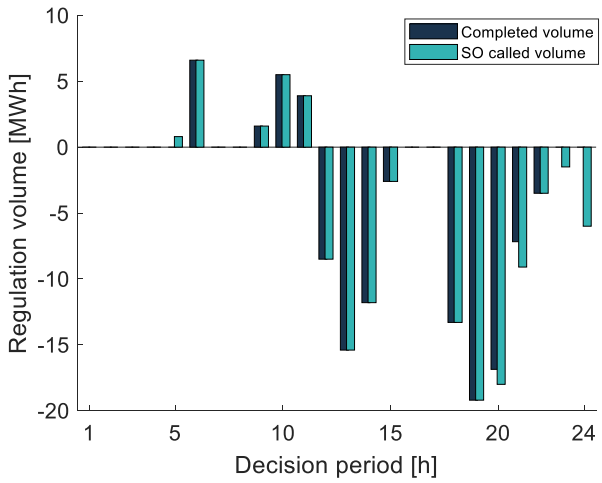

Fig. 14. Reserve response results of the VPP.

It should be noted that such limitations in the VPP's reserve response capability are acceptable in this case study because system security is not involved. If extreme operational scenarios that can severely threaten the system security must be considered, some economically unfavorable approaches such as cutting down the renewable generation and investing in expensive energy storage systems can be adopted to eliminate such limitations.

Although a small-scale VPP is investigated in the case study, the proposed operational regime can be effectively extended for larger VPPs comprise more generators without significantly increasing the computational burden. Table IV gives the averaged computation time for VPPs managing different numbers of generators. As the number of generators is increased from 3 (2 thermal generators and 1 renewable generator) to 40 (20 thermal generators and 20 renewable generators), the total computation time only increases from 1,424s to 1,625s. The reason for this result is two-fold. Firstly, calculating the optimal power generation of the thermal generators does not take too much time. Secondly, increasing the number of renewable generators will not substantially affect the convergence rate of the C&CG algorithm because the number of extreme scenarios for renewable energy production is not changed. Hence, the computational burden increment due to the increased number of generators is not significant compared with the time required to solve the stochastic MMR model.

Table IV
COMPUTATION TIME ANALYSIS

Number of generators	2T 1R	5 T 5 R	10T 10R	20 T 20 R
Computation time	1,424s	1,497s	1,554s	1,625s

T: thermal generator; R: renewable generator

VI. CONCLUSION

This paper proposes an optimal VPP operational regime under reserve uncertainty. In the day-ahead offering stage, the developed price-dependent offering strategy improves the offering flexibility of the VPP in the energy market. Also, the proposed stochastic MMR optimization model utilizes a combination of scenarios and confidence intervals to describe the uncertainties, making it advantageous for problems where some uncertainties have accurate probability distribution while others do not. In the real-time dispatching stage, the proposed self-adaptive algorithm can optimally determine the size of the confidence intervals in a look-back-and-adjust manner. The proposed regime was assessed using the typical day data. The results suggest that the price-dependent offering strategy can increase the VPP profitability in contrast with the price-independent strategy, this effect is most obvious when the real price deviates a lot from the price forecast. Also, the proposed stochastic MMR model can provide less conservative offering decisions compared with the stochastic RO model. Furthermore, by properly determining the size of the confidence intervals, the proposed self-adaptive algorithm significantly reduces the profit loss due to imperfect information in the dispatching stage.

Though all the above conclusions are based on offline analysis, the proposed method is of high potential to be implemented in the future because joint participation in multiple markets and price-dependent bidding strategy are widely adopted in existing electricity markets. Besides, methods that can improve the economic performance of VPPs will be more favorable in practical applications because profitability is the major concern for VPPs.

In the future, several interesting topics can be further investigated, such as the incorporation of flexible loads especially electric vehicles, provision of other types of ancillary services including frequency and voltage regulations.

ACKONWLEDGEMENT

The authors would like to thank the editor and reviewers for their valuable inputs that hugely helped us to improve this work.

This work was supported in part by the National Natural Science Foundation of China (72071100), Guangdong Basic and Applied Basic Research Fund (2019A1515111173), Shenzhen Basic Research Program (JCYJ202103241044100-30), and High-level University Fund (G02236002).

This article has been accepted for publication in a future issue of this journal, but has not been fully edited. Content may change prior to final publication.
Citation information: DOI10.1109/tsg.2022.3153635, IEEE Transactions on Smart Grid

REFERENCES

[1] M. Rahimi, F. J. Ardakani, and A. J. Ardakani, "Optimal stochastic scheduling of electrical and thermal renewable and non-renewable resources in virtual power plant," *Int. J. Electr. Power Energy Syst.*, vol. 127, no. December 2020, p. 106658, 2021, doi: 10.1016/j.ijepes.2020.106658.

[2] J. Qiu, J. Zhao, H. Yang, and Z. Y. Dong, "Optimal Scheduling for Prosumers in Coupled Transactive Power and Gas Systems," *IEEE Trans. Power Syst.*, vol. 33, no. 2, pp. 1970–1980, 2018, doi: 10.1109/TPWRS.2017.2715983.

[3] J. Yang *et al.*, "A Penalty Scheme for Mitigating Uninstructed Deviation of Generation Outputs from Variable Renewables in a Distribution Market," *IEEE Trans. Smart Grid*, vol. 11, no. 5, pp. 4056–4069, 2020, doi: 10.1109/TSG.2020.2993049.

[4] H. Wang, S. Riaz, and P. Mancarella, "Integrated techno-economic modeling, flexibility analysis, and business case assessment of an urban virtual power plant with multi-market co-optimization," *Appl. Energy*, vol. 259, no. September 2019, p. 114142, 2020, doi: 10.1016/j.apenergy.2019.114142.

[5] E. G. Kardakos, C. K. Simoglou, and A. G. Bakirtzis, "Optimal Offering Strategy of a Virtual Power Plant: A Stochastic Bi-Level Approach," *IEEE Trans. Smart Grid*, vol. 7, no. 2, pp. 794–806, 2016, doi: 10.1109/TSG.2015.2419714.

[6] S. Ø. Ottesen, A. Tomasgard, and S. E. Fleten, "Multi market bidding strategies for demand side flexibility aggregators in electricity markets," *Energy*, vol. 149, pp. 120–134, 2018, doi: 10.1016/j.energy.2018.01.187.

[7] S. E. Fleten and T. K. Kristoffersen, "Stochastic programming for optimizing bidding strategies of a Nordic hydropower producer," *Eur. J. Oper. Res.*, vol. 181, no. 2, pp. 916–928, 2007, doi: 10.1016/j.ejor.2006.08.023.

[8] R. E. Hedegaard, T. H. Pedersen, and S. Petersen, "Multi-market demand response using economic model predictive control of space heating in residential buildings," *Energy Build.*, vol. 150, pp. 253–261, 2017, doi: 10.1016/j.enbuild.2017.05.059.

[9] E. K. Aasgård, S. E. Fleten, M. Kaut, K. Midthun, and G. A. Perez-Valdes, "Hydropower bidding in a multi-market setting," *Energy Syst.*, vol. 10, no. 3, pp. 543–565, 2019, doi: 10.1007/s12667-018-0291-y.

[10] S. Sadeghi, H. Jahangir, B. Vatandoust, M. A. Golkar, A. Ahmadian, and A. Elkamel, "Optimal bidding strategy of a virtual power plant in day-ahead energy and frequency regulation markets: A deep learning-based approach," *Int. J. Electr. Power Energy Syst.*, vol. 127, no. November 2020, p. 106646, 2021, doi: 10.1016/j.ijepes.2020.106646.

[11] E. Mashhour and S. M. Moghaddas-Tafreshi, "Bidding strategy of virtual power plant for participating in energy and spinning reserve markets-Part I: Problem formulation," *IEEE Trans. Power Syst.*, vol. 26, no. 2, pp. 949–956, 2011, doi: 10.1109/TPWRS.2010.2070884.

[12] E. Mashhour and S. M. Moghaddas-Tafreshi, "Bidding strategy of virtual power plant for participating in energy and spinning reserve markets-Part II: Numerical analysis," *IEEE Trans. Power Syst.*, vol. 26, no. 2, pp. 957–964, 2011, doi: 10.1109/TPWRS.2010.2070883.

[13] H. Nezamabadi and M. Setayesh Nazar, "Arbitrage strategy of virtual power plants in energy, spinning reserve and reactive power markets," *IET Gener. Transm. Distrib.*, vol. 10, no. 3, pp. 750–763, 2016, doi: 10.1049/iet-gtd.2015.0402.

[14] A. G. Zamani, A. Zakariazadeh, S. Jadid, and A. Kazemi, "Stochastic operational scheduling of distributed energy resources in a large scale virtual power plant," *Int. J. Electr. Power Energy Syst.*, vol. 82, pp. 608–620, 2016, doi: 10.1016/j.ijepes.2016.04.024.

[15] S. Hadayeghparast, A. SoltaniNejad Farsangi, and H. Shayanfar, "Day-ahead stochastic multi-objective economic/emission operational scheduling of a large scale virtual power plant," *Energy*, vol. 172, pp. 630–646, 2019, doi: 10.1016/j.energy.2019.01.143.

[16] A. Baringo, L. Baringo, and J. M. Arroyo, "Day-Ahead Self-Scheduling of a Virtual Power Plant in Energy and Reserve Electricity Markets under Uncertainty," *IEEE Trans. Power Syst.*, vol. 34, no. 3, pp. 1881–1894, 2019, doi: 10.1109/TPWRS.2018.2883753.

[17] M. Vahedipour-Dahraie, H. Rashidizade-Kermani, M. Shafie-khah, and J. P. S. Catalao, "Risk-Averse Optimal Energy and Reserve Scheduling for Virtual Power Plants Incorporating Demand Response Programs," *IEEE Trans. Smart Grid*, vol. 12, no. 2, pp. 1–1, 2020, doi: 10.1109/tsg.2020.3026971.

[18] H. Zhao, B. Wang, Z. Pan, H. Sun, Q. Guo, and Y. Xue, "Aggregating additional flexibility from quick-start devices for multi-energy virtual power plants," *IEEE Trans. Sustain. Energy*, vol. 12, no. 1, pp. 646–658, 2021, doi: 10.1109/TSTE.2020.3014959.

[19] N. Pourghaderi, M. Fotuhi-Firuzabad, M. Moeini-Aghtaie, and M. Kabirifar, "Commercial Demand Response Programs in Bidding of a Technical Virtual Power Plant," *IEEE Trans. Ind. Informatics*, vol. 14, no. 11, pp. 5100–5111, 2018, doi: 10.1109/TII.2018.2828039.

[20] A. Baringo and L. Baringo, "A Stochastic Adaptive Robust Optimization Approach for the Offering Strategy of a Virtual Power Plant," *IEEE Trans. Power Syst.*, vol. 32, no. 5, pp. 3492–3504, 2017, doi: 10.1109/TPWRS.2016.2633546.

[21] F. Sheidaei and A. Ahmarinejad, "Multi-stage stochastic framework for energy management of virtual power plants considering electric vehicles and demand response programs," *Int. J. Electr. Power Energy Syst.*, vol. 120, no. December 2019, p. 106047, 2020, doi: 10.1016/j.ijepes.2020.106047.

[22] M. Jafari and A. Akbari Foroud, "A medium/long-term auction-based coalition-forming model for a virtual power plant based on stochastic programming," *Int. J. Electr. Power Energy Syst.*, vol. 118, no. September 2019, p. 105784, 2020, doi: 10.1016/j.ijepes.2019.105784.

[23] P. L. Jun, DongDong Jun, Nie Linpeng*, "Decision-making Model of Virtual Power Plant for Participating in Spot Market Transaction Based on Hybrid Stochastic and Robust Approach," *Am. J. Environ. Resour. Econ.*, vol. 4, no. 1, p. 32, 2019, doi: 10.11648/j.ajere.20190401.14.

[24] G. Liu, Y. Xu, and K. Tomsovic, "Bidding strategy for microgrid in day-ahead market based on hybrid stochastic/robust optimization," *IEEE Trans. Smart Grid*, vol. 7, no. 1, pp. 227–237, 2016, doi: 10.1109/TSG.2015.2476669.

[25] B. Chen, J. Wang, L. Wang, Y. He, and Z. Wang, "Robust optimization for transmission expansion planning: Minimax cost vs. minimax regret," *IEEE Trans. Power Syst.*, vol. 29, no. 6, pp. 3069–3077, 2014, doi: 10.1109/TPWRS.2014.2313841.

[26] R. Jiang, J. Wang, M. Zhang, and Y. Guan, "Two-stage minimax regret robust unit commitment," *IEEE Trans. Power Syst.*, vol. 28, no. 3, pp. 2271–2282, 2013, doi: 10.1109/TPWRS.2013.2250530.

[27] L. Fan, J. Wang, R. Jiang, and Y. Guan, "Min-max regret bidding strategy for thermal generator considering price uncertainty," *IEEE*

This article has been accepted for publication in a future issue of this journal, but has not been fully edited. Content may change prior to final publication.
Citation information: DOI10.1109/tsg.2022.3153635, IEEE Transactions on Smart Grid

Trans. Power Syst., vol. 29, no. 5, pp. 2169–2179, 2014, doi: 10.1109/TPWRS.2014.2308477.

[28] M. Shafiekhani, A. Badri, M. Shafie-khah, and J. P. S. Catalão, "Strategic bidding of virtual power plant in energy markets: A bi-level multi-objective approach," *Int. J. Electr. Power Energy Syst.*, vol. 113, no. December 2018, pp. 208–219, 2019, doi: 10.1016/j.ijepes.2019.05.023.

[29] S. R. Dabbagh and M. K. Sheikh-El-Eslami, "Risk-based profit allocation to DERs integrated with a virtual power plant using cooperative Game theory," *Electr. Power Syst. Res.*, vol. 121, pp. 368–378, 2015, doi: 10.1016/j.epsr.2014.11.025.

[30] X. Kong, J. Xiao, D. Liu, J. Wu, C. Wang, and Y. Shen, "Robust stochastic optimal dispatching method of multi-energy virtual power plant considering multiple uncertainties," *Appl. Energy*, vol. 279, no. May, p. 115707, 2020, doi: 10.1016/j.apenergy.2020.115707.

[31] H. PandŽić, J. M. Morales, A. J. Conejo, and I. Kuzle, "Offering model for a virtual power plant based on stochastic programming," *Appl. Energy*, vol. 105, pp. 282–292, 2013, doi: 10.1016/j.apenergy.2012.12.077.

[32] P. J. M. Interconnection, "https://www.pjm.com/markets-and-operations." .

[33] J. Ma, M. Yang, X. Han, and Z. Li, "Ultra-short-term wind generation forecast based on multivariate empirical dynamic modeling," *2017 IEEE Ind. Appl. Soc. Annu. Meet. IAS 2017*, vol. 2017-Janua, no. 2, pp. 1–8, 2017, doi: 10.1109/IAS.2017.8101715.

[34] J. Tastu1 and H. M. and H. A. N. , Pierre Pinson1, Ewelina Kotwa1, "Spatio-temporal analysis and modeling of short-term wind power forecast errors," *Wind Energy*, no. April 2010, pp. 1–20, 2013, doi: 10.1002/we.

[35] B. Zeng and L. Zhao, "Solving two-stage robust optimization problems using a column-and- constraint generation method," *Oper. Res. Lett.*, vol. 41, no. 5, pp. 457–461, 2013, doi: 10.1016/j.orl.2013.05.003.

[36] NORDPOOL, "https://www.nordpoolgroup.com/." .

[37] FINGRID, "https://data.fingrid.fi/open-data-forms/search/en/?selected_datasets=181." .

[38] Y. Jia, X. Lyu, C. S. Lai, Z. Xu, and M. Chen, "A retroactive approach to microgrid real-time scheduling in quest of perfect dispatch solution," *J. Mod. Power Syst. Clean Energy*, vol. 7, no. 6, pp. 1608–1618, 2019, doi: 10.1007/s40565-019-00574-2.